Supplement of Atmos. Chem. Phys., 18, 11507–11527, 2018
https://doi.org/10.5194/acp-18-11507-2018-supplement
© Author(s) 2018. This work is distributed under
the Creative Commons Attribution 4.0 License.

Atmospheric Chemistry and Physics
Open Access
EGU

Supplement of

Black carbon-induced snow albedo reduction over the Tibetan Plateau: uncertainties from snow grain shape and aerosol–snow mixing state based on an updated SNICAR model

Cenlin He et al.

Correspondence to: Cenlin He (cenlinhe@ucar.edu)

The copyright of individual parts of the supplement might differ from the CC BY 4.0 License.

Table S1. Summary of observed BC concentrations in snow over the Tibetan Plateau.

Region	Site	Lat. (°N)	Lon. (°N)	Elev. (m)	Year	Season/ Month	Sample type	BC conc. (ppb)	Snow depth (cm)	Snow density (kg/m^3)	Data sources
Himalayas (HIMA)	Mera Glacier	27.72	86.87	6376	2000-2010	monsoon	ice core	3.28			Ginot et al. 2014
	Mera Glacier	27.72	86.87	6376	2000-2010	non-monsoon	ice core	18.31			Ginot et al. 2014
	Mera Glacier	27.72	86.87	6376	2000-2010	annual	ice core	11.89			Ginot et al. 2014
	Khumbu Valley	27.96	86.8	5079-5700	2009-2012	monsoon	surface snow	1.15			Jacobi et al. 2015
	Khumbu Valley	27.96	86.8	5079-5700	2009-2012	non-monsoon	surface snow	5.89	43.2		Jacobi et al. 2015
	Khumbu Valley	27.96	86.8	5079-5700	2009-2012	annual	surface snow	5.46			Jacobi et al. 2015
	Mera Glacier	27.45	86.88	5400-6400	2009	spring	snowpit	68.47	>100	600	Kaspari et al. 2014
	Sunderdhunga	30.02	79.85	4869-5008	2015	post-monsoon	snowpit	150.15	120		Svensson et al. 2018
	East Rongbuk glacier	28.03	86.96	6518	2000	annual	ice core	0.29			Kaspari et al. 2011
	East Rongbuk glacier	28.03	86.94	6350	2013	May	snowpit	11	120		Li et al. 2016a
	East Rongbuk glacier	28.02	86.96	6500	2000-2001	monsoon	ice core	33.72			Ming et al. 2008
	East Rongbuk glacier	28.02	86.96	6500	2000-2001	non-monsoon	ice core	21.5			Ming et al. 2008
	East Rongbuk glacier	28.02	86.96	6500	2000-2001	annual	ice core	26.43			Ming et al. 2008
	East Rongbuk glacier	28.02	86.96	6465	2004	Oct.	snowpit	18	100		Ming et al. 2009a
	East Rongbuk glacier	28.02	86.96	6517	2007	Apr.-May	surface snow	54.11		480	Ming et al. 2012
	East Rongbuk glacier	28.02	86.96	6500	2006	Sept.	snowpit	9			Ming et al. 2013
	East Rongbuk glacier	28.02	86.96	6500	2000-2004	annual	ice core	10.4			Xu et al. 2009b
	Thorung Glacier	28.79	83.93	5410	2012	Jun.	snowpit	19	42		Li et al. 2016a
	Qiangyong Glacier	28.83	90.25	5400	2001	summer	surface snow	43.1			Xu et al. 2006
	Qiangyong Glacier	28.86	90.23	5739	2014	May	snowpit	28	155		Li et al. 2016a
	Kangwure	28.47	85.82	6000	2001	summer	surface snow	21.8			Xu et al. 2006
	Namunani	30.45	81.27	6080–5780	2004	summer	surface snow	4.34			Xu et al. 2006
	Noijin Kangsang glacier	29.04	90.2	5950	2000-2006	annual	ice core	20.49			Xu et al. 2009b
	TP-S-1511-6	29.19	90.62	4762	2015	Nov.	surface snow	251	6.8		Zhang et al. 2018
	TP-S-1511-8	27.39	88.83	4150	2015	Nov.	surface snow	575	5	275	Zhang et al. 2018
	TP-S-1511-9	28.82	87.93	4851	2015	Nov.	surface snow	3417	12.5	230	Zhang et al. 2018

	TP-S-1511-16	29	87.47	4798	2015	Nov.	surface snow	887	9	300	Zhang et al. 2018
	TP-S-1511-17	28.96	87.44	5163	2015	Nov.	surface snow	822	15	270	Zhang et al. 2018
	TP-S-1511-18	28.91	87.43	5042	2015	Nov.	surface snow	1278	8	250	Zhang et al. 2018
	TP-S-1511-21	28.67	86.13	4565	2015	Nov.	surface snow	1079	9	200	Zhang et al. 2018
	TP-S-1511-22	28.52	86.17	5096	2015	Nov.	surface snow	2201	5	200	Zhang et al. 2018
	TP-S-1511-23	28.65	86.08	4592	2015	Nov.	surface snow	1072	9	325	Zhang et al. 2018
	TP-S-1511-24	28.76	85.66	4614	2015	Nov.	surface snow	1042	14	250	Zhang et al. 2018
	TP-S-1511-25	28.9	85.4	4861	2015	Nov.	surface snow	932	11.5	225	Zhang et al. 2018
	TP-S-1511-26	28.93	85.4	5166	2015	Nov.	surface snow	759	12	275	Zhang et al. 2018
	TP-S-1511-27	29.83	92.34	4971	2015	Nov.	surface snow	3587	17	150	Zhang et al. 2018
	TP-S-1511-28	29.63	94.63	4304	2015	Nov.	surface snow	952	12	200	Zhang et al. 2018
	TP-S-1511-29	29.61	94.67	4523	2015	Nov.	surface snow	256	24	200	Zhang et al. 2018
	MYL	30.11	83.39	4610	2014	Dec.	surface snow	320	11		Zhang et al. 2018
Central Tibetan Plateau (CTP)	Zhadang Glacier	30.47	90.64	5570-5790	2014-2015	Aug.-Sept.	surface snow	140.9	138	290	Li et al. 2018
	Zhadang Glacier	30.47	90.64	5570-5790	2015	May	surface snow	627.38	138	290	Li et al. 2018
	Zhadang Glacier	30.47	90.65	5800	2013-2014	Jun., Aug.	snowpit	49.02	150		Li et al. 2016a
	Zhadang Glacier	30.48	90.65	5500-5800	2012	Jul.-Aug.	surface snow	120.52	5	200-400	Qu et al. 2014
	Zhadang Glacier	30.47	90.5	5800	2006	Jul.	snowpit	87.4	40		Ming et al. 2009a
	XiaoDongkemadi Glacier	33.08	92.07	5450-5750	2014-2015	Aug.	surface snow	40.99	15	200	Li et al. 2017
	XiaoDongkemadi Glacier	33.08	92.07	5450-5750	2015	May	surface snow	42.66	34	350	Li et al. 2017
	Xiaodongkemadi Glacier	33.07	92.09	5742	2014	May	snowpit	29	100		Li et al. 2016a
	Xiaodongkemadi Glacier	33.07	92.09	5742	2014	Jul.	snowpit	15.57	100		Li et al. 2016a
	La'nong	30.42	90.57	5850	2005	Jun.	snowpit	67.33	28		Ming et al. 2009a
	Meikuang	35.67	94.18	5200	2005	Nov.	snowpit	81		150	Ming et al. 2009b
	Meikuang	35.67	94.18	5200	2001	summer	surface snow	446			Xu et al. 2006
	Dongkemadi	33.1	92.08	5600	2001	summer	snowpit	79.25	52		Xu et al. 2006
	Dongkemadi	33.1	92.08	5600	2005	summer	surface snow	36			Ming et al. 2013
	Tanggula glacier	33.11	92.09	5800	2000-2004	annual	ice core	43.56			Xu et al., 2009b

	TP-S-1511-1	30.45	91.05	4216	2015	Nov.	surface snow	1283	3		Zhang et al. 2018
	TP-S-1511-2	30.67	91.1	5036	2015	Nov.	surface snow	469	6.8		Zhang et al. 2018
	TP-S-1511-3	30.68	91.1	5124	2015	Nov.	surface snow	5093	9		Zhang et al. 2018
	TP-S-1511-4	30.79	90.96	4687	2015	Nov.	surface snow	4193	5		Zhang et al. 2018
	TP-S-1511-5	30.68	91.1	5096	2015	Nov.	surface snow	1085	17.1		Zhang et al. 2018
	24K	30.99	91.68	5100	2014	Dec.	surface snow	877	11		Zhang et al. 2018
	NMC	30.75	91.68	4729	2014	Dec.	surface snow	601	11		Zhang et al. 2018
	TGL	32.9	91.92	5163	2014	Dec.	surface snow	1014	11		Zhang et al. 2018
Northwestern Tibetan Plateau (NWTP)	Muztagh Ata	38.29	75.02	6250-7000	2000	annual	ice core	39.49			Liu et al. 2008
	Abramov 1	39.59	71.56	4235-4390	2013-2014	Aug.	snowpit	248.90	161		Schmale et al. 2017
	Abramov 2	39.62	71.52	4275	2013	Aug.	snowpit	249.55	99		Schmale et al. 2017
	Mt. Muztagh Ata	38.28	75.07	6500	2000	annual	ice core	1.32			Wang et al. 2015
	Mt. Muztagh Ata	38.28	75.02	6350	2001	summer	snowpit	52.08	180		Xu et al. 2006
	Mt. Muztagh Ata	38.28	75.1	6300	2000	annual	ice core	39.2			Xu et al. 2009b
	Muji Glacier	39.19	73.74	4760-5150	2012	Jul.-Sept.	surface snow	318.11	36		Yang et al. 2015
	Muji Glacier	39.19	73.74	4760-5150	2012	Oct.	surface snow	64.69	36		Yang et al. 2015
	Muji Glacier	39.19	73.74	5230-5530	2012	Jul.-Sept.	surface snow	235.13	110		Yang et al. 2015
	Muji Glacier	39.19	73.74	5230-5530	2012	Oct.	surface snow	61.09	110		Yang et al. 2015
Northeastern Tibetan Plateau (NETP)	Laohugou Glacier No.12	39.43	96.56	5026	2014	May	snowpit	133	40		Li et al. 2016a
	Laohugou Glacier No.12	39.43	96.56	5026	2014	Aug.	snowpit	15.32	40		Li et al. 2016a
	Laohugou Glacier No.12	39.17-39.58	96.17-96.58	4450-4950	2013-2014	Jul.-Aug.	surface snow	261.93	9	333	Li et al. 2016b
	Laohugou Glacier No.12	39.43	96.56	5045	2005	Oct.	snowpit	35.5	30		Ming et al. 2009a
	Laohugou Glacier No.12	39.50	96.52	4350-4600	2015-2016	Dec., Mar.	surface snow	2941.67	>5		Zhang et al. 2017b
	Laohugou Glacier No.12	39.46	96.55	4600-4850	2015-2016	Jun., Aug.	surface snow	1215.35	>5		Zhang et al. 2017b
	Laohugou Glacier No.12	39.5	96.52	4250	2015	Dec.	surface snow	1483.7	20		Zhang et al. 2018
	Qiyi	39.23	97.06	4850	2005	Jul.	snowpit	22.5	34		Ming et al. 2009a

	July 1st	39.23	97.75	4600	2001	summer	surface snow	52.64			Xu et al. 2006
	RYS	36.5	101.52	3396	2014	Dec.	surface snow	8923	11		Zhang et al. 2018
	TP-S-1511-35	34.11	97.65	4781	2015	Nov.	surface snow	4217	10	325	Zhang et al. 2018
	TP-S-1511-36	35.44	98.65	4363	2015	Nov.	surface snow	3098	11	300	Zhang et al. 2018
	TP-S-1511-37	35.37	99.29	4297	2015	Nov.	surface snow	7373	16	250	Zhang et al. 2018
	TP-S-1511-38	35.39	99.31	4298	2015	Dec.	surface snow	4122	18	225	Zhang et al. 2018
	TP-S-1511-39	35.51	99.51	4405	2015	Dec.	surface snow	2895	14	225	Zhang et al. 2018
	MD1	34.86	98.17	4220	2014	Dec.	surface snow	3123	11		Zhang et al. 2018
	TP-S-1511-34	33.61	97.24	4366	2015	Nov.	surface snow	4009	12	350	Zhang et al. 2018
Southeastern Tibetan Plateau (SETP)	Yulong Glacier	27.1	100.2	4606	2014	May	snowpit	34	170		Li et al. 2016a
	Yulong Glacier	27.1	100.2	4700	2015	Apr.-Jun.	snowpit	281.32	80	440	Niu et al. 2017a
	Yulong Glacier	27.1	100.2	4700	2015	May-Aug.	surface snow	698.09	80	423	Niu et al. 2017a
	Palong-Zanbu No. 4 Glacier	29.21	96.92	5500	2000-2005	monsoon	ice core	5.88			Xu et al. 2009a
	Palong-Zanbu No. 4 Glacier	29.21	96.92	5500	2000-2005	non-monsoon	ice core	12.92			Xu et al. 2009a
	Palong-Zanbu No. 4 Glacier	29.21	96.92	5500	2000-2005	annual	ice core	9.68			Xu et al. 2009b
	Zuoqiupu glacier	29.21	96.92	5600	2000-2006	monsoon	ice core	4.56			Xu et al. 2009b
	Zuoqiupu glacier	29.21	96.92	5600	2000-2006	non-monsoon	ice core	11.22			Xu et al. 2009b
	Zuoqiupu glacier	29.21	96.92	5600	2000-2006	annual	ice core	8.31			Xu et al. 2009b
	Yarlong	29.31	96.77	4030-4124	2015	Jun.	surface snow	79.7		300	Zhang et al. 2017a
	Dongga	29.23	96.88	4570-4705	2015	Jun.	snowpit	97.3	115	300	Zhang et al. 2017a
	Renlongba	29.25	96.92	4740-4854	2015	Jun.	snowpit	318	70	300	Zhang et al. 2017a
	Demula Glacier	29.35	97.02	5000-5200	2015	Jun.	snowpit	125	80	300	Zhang et al. 2017a
	Demula Glacier	29.36	97.02	5404	2014	May	snowpit	17	180		Li et al. 2016a
	TP-S-1511-30	29.77	95.7	3728	2015	Nov.	surface snow	1343	11	400	Zhang et al. 2018
	TP-S-1511-31	29.26	96.94	4582	2015	Nov.	surface snow	2117	12	250	Zhang et al. 2018
	TP-S-1511-32	29.32	97.03	4745	2015	Nov.	surface snow	202	20	175	Zhang et al. 2018
	LWQ1	31.22	96.57	4370	2014	Dec.	surface snow	1735	11		Zhang et al. 2018

North of Tibetan Plateau (NOTP)	Miao'ergou No.3	43.06	94.32	4510	2005	Aug.	snowpit	111	70		Ming et al. 2009a
	Haxilegen River No.48	43.73	84.46	3755	2006	Oct.	snowpit	46.86	90		Ming et al. 2009a
	Urumqi Riverhead No.1	43.1	86.82	4050	2006	Nov.	snowpit	141			Ming et al. 2009b
	Urumqi Riverhead No.1	43.11	86.81	3845-4050	2013	Aug.	surface snow	97.79	100	294	Ming et al. 2016
	Urumqi glacier no.1	43.01	86.82	4130	2004-2005	monsoon	surface snow	281.86	150		Xu et al. 2012
	Urumqi glacier no.1	43.01	86.82	4130	2004-2005	non-monsoon	surface snow	79.36	200		Xu et al. 2012
	Urumqi glacier no.1	43.01	86.82	4130	2004-2005	annual	surface snow	157.25	175		Xu et al. 2012
	Suek	41.78	77.75	4325-4473	2013-2014	Aug.	snowpit	426.33	135		Schmale et al. 2017
	No. 354	41.8	78.18	4325-4355	2013-2014	Aug.	snowpit	564.16	102		Schmale et al. 2017
	Golubin	42.44	74.51	4116	2014	Aug.	snowpit	730.58	120		Schmale et al. 2017

Table S2. Regional and seasonal mean all-sky surface downward solar radiation and cloud cover fraction over the Tibetan Plateau during 2000–2015 from the MERRA-2 reanalysis data.

Season	Variable	Region[1]					
		HIMA	**CTP**	**NWTP**	**NETP**	**SETP**	**NOTP**
monsoon	surface downward solar flux (W m^{-2})	289.8	314.0	321.8	284.3	267.3	280.4
	cloud cover fraction	0.413	0.362	0.203	0.406	0.503	0.311
non-monsoon	surface downward solar flux (W m^{-2})	245.0	226.6	193.8	203.6	217.6	166.5
	cloud cover fraction	0.255	0.387	0.455	0.379	0.376	0.434
annual	surface downward solar flux (W m^{-2})	259.9	255.7	236.5	230.5	234.2	204.5
	cloud cover fraction	0.308	0.379	0.371	0.388	0.418	0.393

[1]Sub-regions: Himalayas (HIMA), central Tibetan Plateau (CTP), northwestern Tibetan Plateau (NWTP), northeastern Tibetan Plateau (NETP), southeastern Tibetan Plateau (SETP), and north of Tibetan Plateau (NOTP).

Table S3. Regional and seasonal mean BC-induced all-sky snow albedo reductions for aged snow over the Tibetan Plateau during 2000–2015. See Table 2 for results of fresh snow.

Region[1]		Season	BC mean content (ppb)	Aged snow (R_e = 1000 μm)							
				External mixing				Internal mixing			
				Sphere	Spheroid	Hexagonal plate	Koch snowflake	Sphere	Spheroid	Hexagonal plate	Koch snowflake
HIMA	high alt.	monsoon	16.3	0.010	0.010	0.009	0.008	0.014	0.014	0.012	0.012
	low alt.										
	high alt.	non-monsoon	29.4	0.024	0.022	0.018	0.017	0.030	0.028	0.023	0.022
	low alt.		1151.8	0.112	0.110	0.105	0.102	0.169	0.166	0.158	0.153
	high alt.	annual	17.5	0.015	0.014	0.012	0.011	0.020	0.019	0.016	0.015
	low alt.										
CTP	high alt.	monsoon	63.2	0.032	0.030	0.026	0.025	0.042	0.040	0.035	0.033
	low alt.		446.0	0.120	0.112	0.097	0.090	0.163	0.152	0.132	0.123
	high alt.	non-monsoon	331.6	0.091	0.084	0.072	0.067	0.122	0.113	0.097	0.090
	low alt.		1632.9	0.130	0.128	0.122	0.119	0.193	0.190	0.181	0.176
	high alt.	annual	146.3	0.056	0.051	0.044	0.041	0.074	0.068	0.058	0.054
	low alt.		263.5	0.087	0.081	0.070	0.066	0.117	0.109	0.095	0.089
NWTP	high alt.	monsoon	143.6	0.064	0.059	0.050	0.046	0.083	0.076	0.065	0.060
	low alt.		272.2	0.095	0.088	0.075	0.069	0.126	0.116	0.100	0.093
	high alt.	non-monsoon	61.1	0.041	0.037	0.031	0.029	0.051	0.047	0.040	0.037
	low alt.		64.7	0.032	0.030	0.027	0.026	0.042	0.040	0.036	0.034
	high alt.	annual	87.4	0.047	0.043	0.036	0.034	0.061	0.055	0.047	0.043
	low alt.		191.4	0.070	0.066	0.057	0.054	0.095	0.088	0.077	0.072
NETP	high alt.	monsoon									
	low alt.		190.9	0.054	0.051	0.045	0.042	0.074	0.070	0.061	0.058
	high alt.	non-monsoon									
	low alt.		4323.2	0.287	0.279	0.260	0.249	0.393	0.385	0.364	0.352
	high alt.	annual									
	low alt.		823.0	0.164	0.153	0.134	0.125	0.225	0.212	0.186	0.174
SETP	high alt.	monsoon	5.2	0.005	0.005	0.004	0.004	0.008	0.008	0.007	0.007
	low alt.		263.6	0.087	0.080	0.068	0.063	0.115	0.106	0.091	0.084
	high alt.	non-monsoon	13.7	0.016	0.014	0.012	0.011	0.020	0.018	0.015	0.014
	low alt.		1110.9	0.128	0.124	0.115	0.111	0.187	0.182	0.168	0.161
	high alt.	annual	9.0	0.011	0.010	0.009	0.008	0.015	0.013	0.011	0.011
	low alt.		249.4	0.087	0.080	0.068	0.062	0.114	0.105	0.089	0.083
NOTP	high alt.	monsoon									
	low alt.		368.6	0.109	0.100	0.085	0.079	0.145	0.133	0.114	0.106
	high alt.	non-monsoon									
	low alt.		89.1	0.051	0.046	0.039	0.036	0.065	0.059	0.050	0.046
	high alt.	annual									
	low alt.		138.3	0.068	0.062	0.052	0.048	0.088	0.080	0.068	0.063

[1]Sub-regions: Himalayas (HIMA), central Tibetan Plateau (CTP), northwestern Tibetan Plateau (NWTP), northeastern Tibetan Plateau (NETP), southeastern Tibetan Plateau (SETP), and north of Tibetan Plateau (NOTP). Each sub-region is further divided into high (>5200 m) and low (<5200 m) altitudes.

Table S4. Regional and seasonal mean BC-induced all-sky surface radiative effects (W m^{-2}) for aged snow over the Tibetan Plateau during 2000–2015. See Table 3 for results of fresh snow.

Region[1]		Season	Aged snow (R_e = 1000 μm)							
			External mixing				Internal mixing			
			Sphere	Spheroid	Hexagonal plate	Koch snowflake	Sphere	Spheroid	Hexagonal plate	Koch snowflake
HIMA	high alt.	monsoon	2.9	2.8	2.5	2.4	4.1	3.9	3.6	3.4
	low alt.									
	high alt.	non-monsoon	5.8	5.3	4.5	4.1	7.4	6.8	5.7	5.3
	low alt.		27.3	27.0	25.8	25.0	41.4	40.8	38.7	37.4
	high alt.	annual	4.0	3.7	3.2	3.0	5.2	4.9	4.2	3.9
	low alt.									
CTP	high alt.	monsoon	9.9	9.4	8.3	7.8	13.2	12.4	10.9	10.3
	low alt.		37.7	35.1	30.4	28.4	51.3	47.8	41.5	38.7
	high alt.	non-monsoon	20.7	19.1	16.3	15.1	27.6	25.5	22.0	20.4
	low alt.		29.5	29.1	27.7	26.9	43.7	43.1	41.1	39.8
	high alt.	annual	14.3	13.2	11.3	10.5	18.8	17.4	14.9	13.9
	low alt.		22.2	20.7	18.0	16.8	30.0	28.0	24.3	22.7
NWTP	high alt.	monsoon	20.7	18.9	15.9	14.7	26.7	24.5	20.8	19.2
	low alt.		30.5	28.2	24.1	22.3	40.6	37.4	32.1	29.8
	high alt.	non-monsoon	7.9	7.2	6.1	5.6	10.0	9.1	7.7	7.1
	low alt.		6.1	5.8	5.2	5.0	8.2	7.8	6.9	6.5
	high alt.	annual	11.2	10.2	8.6	7.9	14.3	13.1	11.1	10.2
	low alt.		16.5	15.5	13.6	12.7	22.3	20.9	18.2	17.0
NETP	high alt.	monsoon								
	low alt.		15.2	14.4	12.8	12.0	21.0	19.8	17.5	16.4
	high alt.	non-monsoon								
	low alt.		58.4	56.9	52.9	50.7	79.9	78.4	74.2	71.6
	high alt.	annual								
	low alt.		37.7	35.3	30.9	28.9	52.0	48.8	42.9	40.2
SETP	high alt.	monsoon	1.4	1.3	1.2	1.1	2.2	2.1	1.9	1.8
	low alt.		23.3	21.4	18.2	16.9	30.7	28.3	24.2	22.5
	high alt.	non-monsoon	3.5	3.1	2.6	2.4	4.4	4.0	3.4	3.1
	low alt.		27.8	27.0	25.1	24.1	40.8	39.5	36.7	35.1
	high alt.	annual	2.6	2.4	2.0	1.9	3.4	3.2	2.7	2.5
	low alt.		20.4	18.7	15.8	14.6	26.8	24.6	20.9	19.4
NOTP	high alt.	monsoon								
	low alt.		30.5	28.1	23.9	22.1	40.5	37.4	32.0	29.7
	high alt.	non-monsoon								
	low alt.		8.5	7.7	6.5	6.0	10.8	9.9	8.3	7.7
	high alt.	annual								
	low alt.		14.0	12.8	10.7	9.9	18.0	16.4	13.9	12.8

[1]Sub-regions: Himalayas (HIMA), central Tibetan Plateau (CTP), northwestern Tibetan Plateau (NWTP), northeastern Tibetan Plateau (NETP), southeastern Tibetan Plateau (SETP), and north of Tibetan Plateau (NOTP). Each sub-region is further divided into high (>5200 m) and low (<5200 m) altitudes.

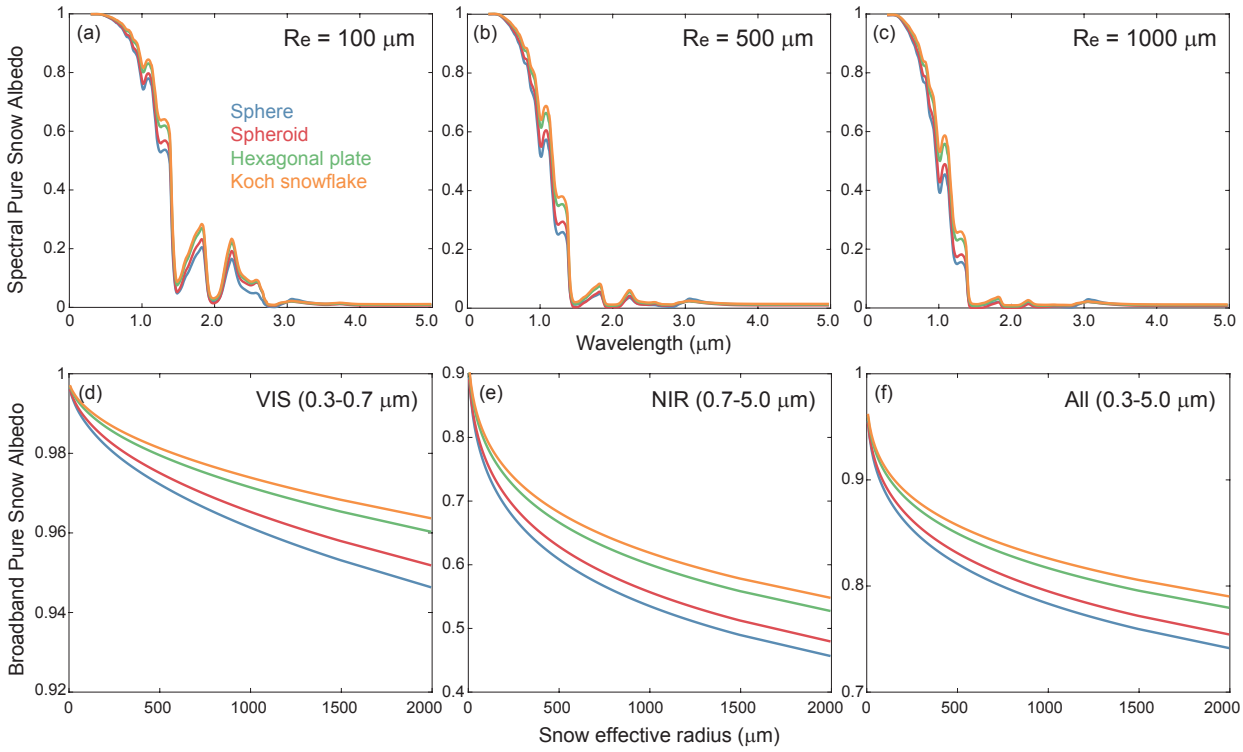

Figure S1. (a–c) Spectral (0.3–5 μm) diffuse albedo of pure semi-infinite snow layers with effective radii (R_e) of (a) 100, (b) 500, and (c) 1000 μm for sphere (blue), spheroid (red), hexagonal plate (green), and Koch snowflake (orange) based on the updated SNICAR model. (d–f) Same as (a–c), but for broadband diffuse pure snow albedo as a function of snow effective radius (R_e) at (d) visible (VIS, 0.3–0.7 μm), (e) near-infrared (NIR, 0.7–5 μm), and (f) all (0.3–5 μm) wavelengths.

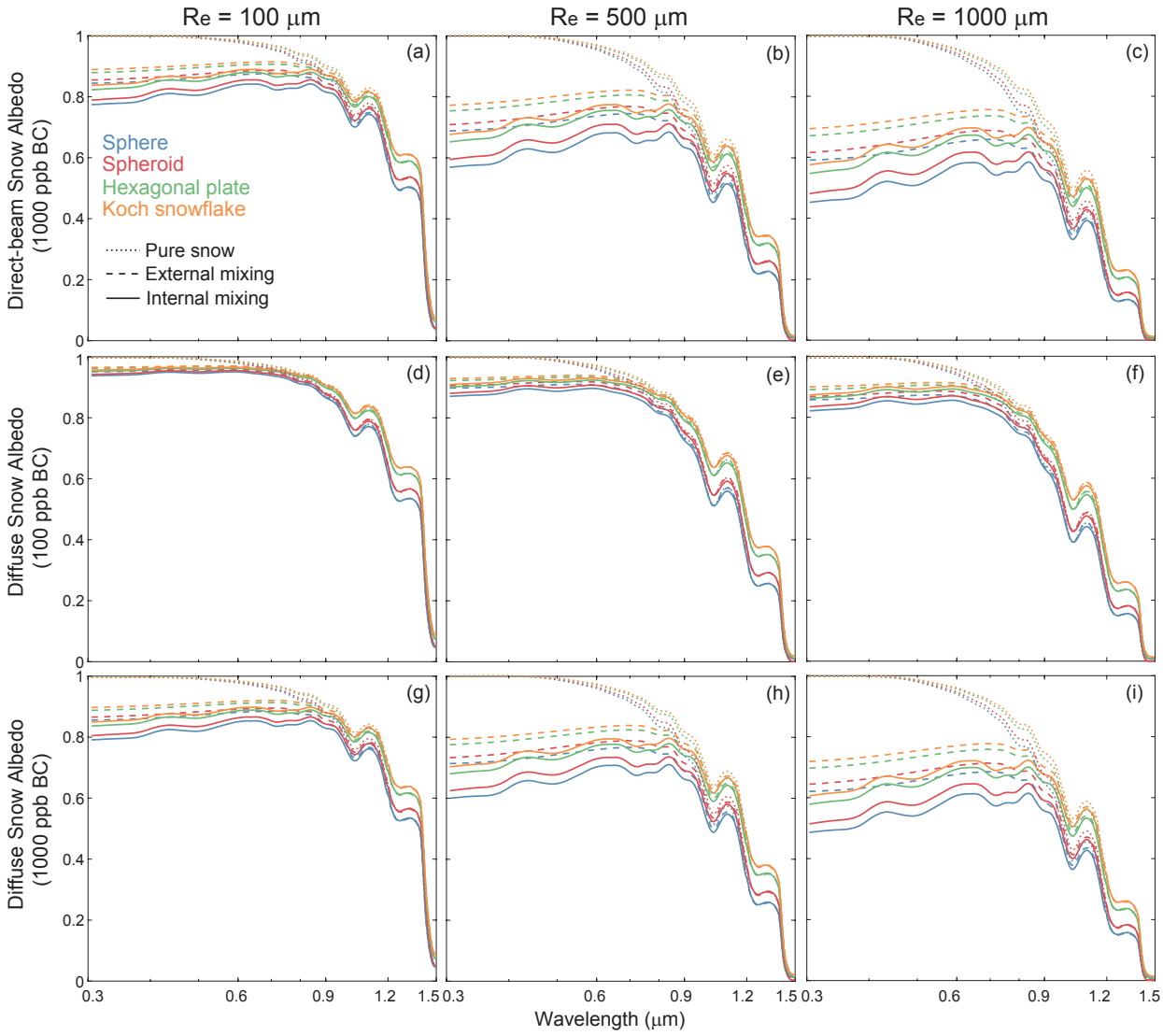

Figure S2. Spectral (a–c) direct-beam and (d–i) diffuse albedos of semi-infinite snow layers with effective radii (R_e) of (a,d,g) 100, (b,e,h) 500, and (c,f,i) 1000 μm for pure snow (dotted lines), snow externally mixed with BC (dashed lines), and snow internally mixed with BC (solid lines) with shapes of sphere (blue), spheroid (red), hexagonal plate (green), and Koch snowflake (orange) for (d–f) 100 and (a–c, g–i) 1000 ppb BC based on the updated SNICAR model.

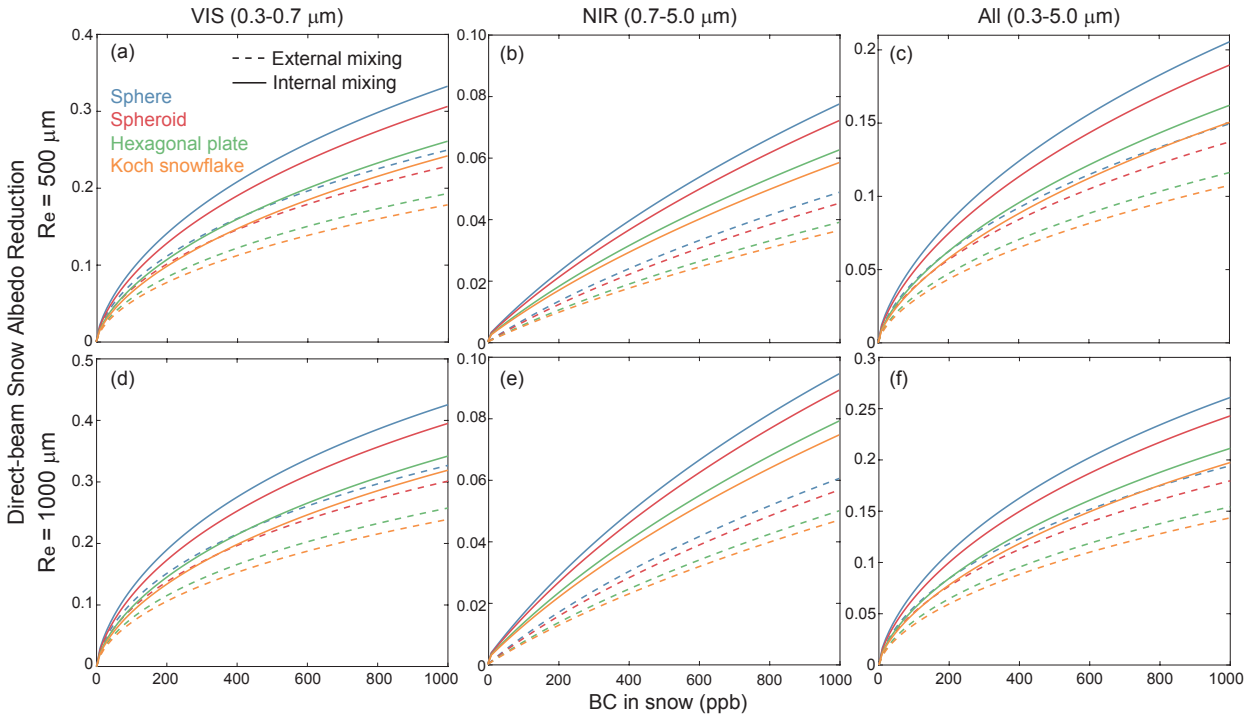

Figure S3. Broadband direct-beam snow albedo reduction as a function of BC concentration in semi-infinite snow layers with effective radii (R_e) of (a–c) 500 and (d–f) 1000 μm at (a,d) visible (VIS, 0.3–0.7 μm), (b,e) near-infrared (NIR, 0.7–5 μm), and (c,f) all (0.3–5 μm) wavelengths for BC-snow external snow externally (dashed lines) and internal mixing (solid lines) with shapes of sphere (blue), spheroid (red), hexagonal plate (green), and Koch snowflake (orange) based on the updated SNICAR model.

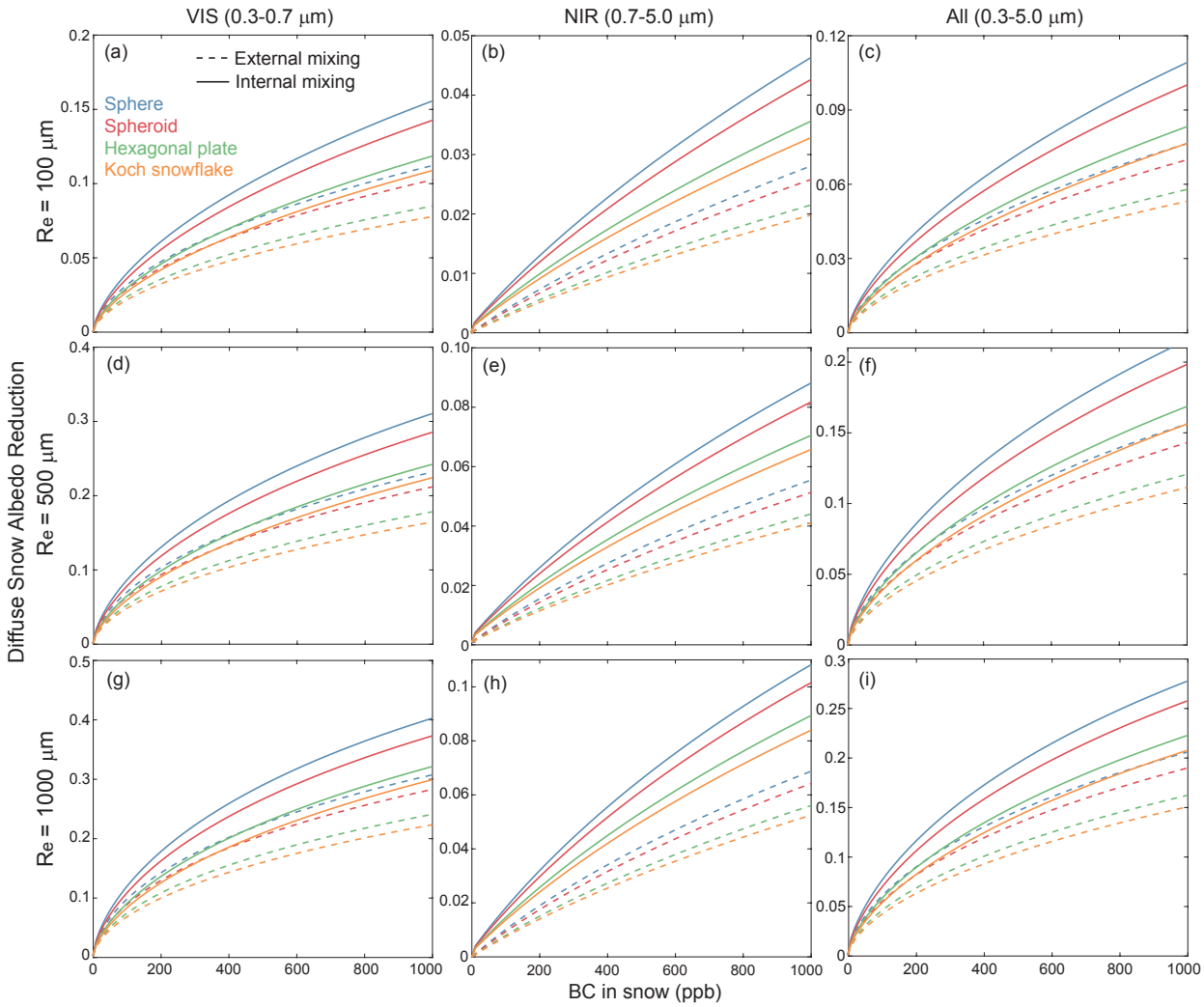

Figure S4. Broadband diffuse snow albedo reduction as a function of BC concentration in semi-infinite snow layers with effective radii (R_e) of (a–c) 100, (d–f) 500, and (g–i) 1000 μm at (a,d,g) visible (VIS, 0.3–0.7 μm), (b,e,h) near-infrared (NIR, 0.7–5 μm), and (c,f,i) all (0.3–5 μm) wavelengths for BC-snow external snow externally (dashed lines) and internal mixing (solid lines) with shapes of sphere (blue), spheroid (red), hexagonal plate (green), and Koch snowflake (orange) based on the updated SNICAR model.

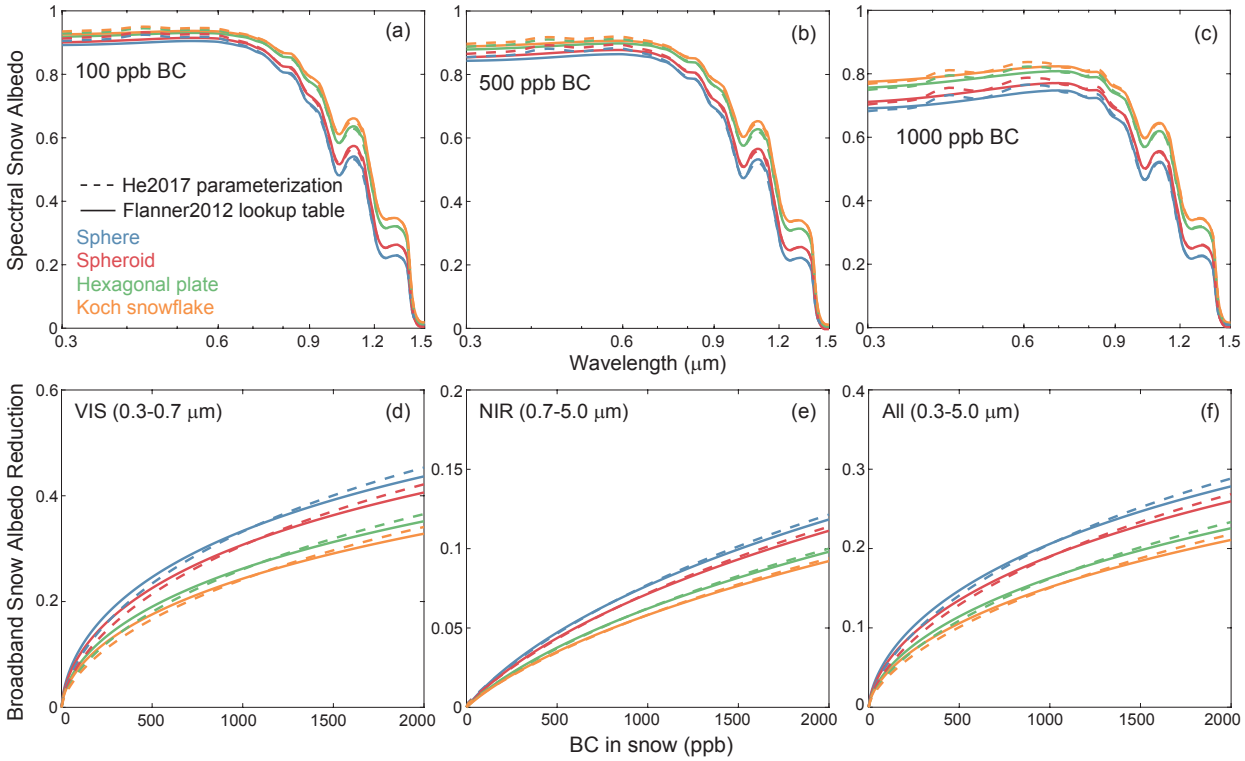

Figure S5. Comparisons of SNICAR simulated direct-beam albedos of semi-infinite snow layers between using the Flanner et al. (2012) lookup table (solid lines) and the He et al. (2017b) parameterization (dashed lines) for BC internally mixed with snow grains with an effective radius of 500 μm for sphere (blue), spheroid (red), hexagonal plate (green), and Koch snowflake (orange). (a–c) Spectral (0.3–1.5 μm) snow albedo for BC concentrations of (a) 100, (b) 500, and (c) 1000 ppb. (d–f) Broadband snow albedo reduction as a function of BC concentration in snow at (d) visible (VIS, 0.3–0.7 μm), (e) near-infrared (NIR, 0.7–5 μm), and (f) all (0.3–5 μm) wavelengths.

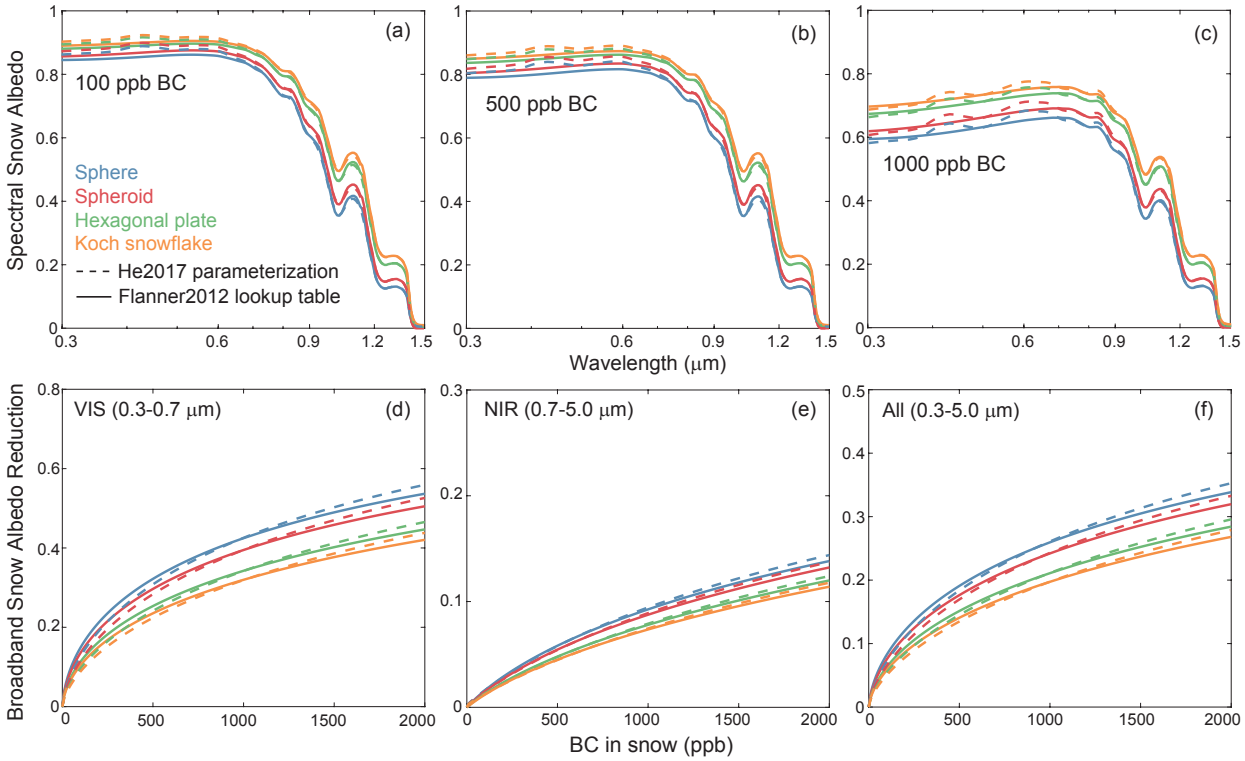

Figure S6. Same as Fig. S5, but for snow grains with an effective radius of 1000 μm.

References

Ginot, P., Dumont, M., Lim, S., Patris, N., Taupin, J.-D., Wagnon, P., Gilbert, A., Arnaud, Y., Marinoni, A., Bonasoni, P., and Laj, P.: A 10 year record of black carbon and dust from a Mera Peak ice core (Nepal): variability and potential impact on melting of Himalayan glaciers, The Cryosphere, 8, 1479–1496, doi:10.5194/tc-8-1479-2014, 2014.

Jacobi, H.-W., Lim, S., Ménégoz, M., Ginot, P., Laj, P., Bonasoni, P., Stocchi, P., Marinoni, A., and Arnaud, Y.: Black carbon in snow in the upper Himalayan Khumbu Valley, Nepal: observations and modeling of the impact on snow albedo, melting, and radiative forcing, The Cryosphere, 9, 1685–1699, doi:10.5194/tc-9-1685-2015, 2015.

Kaspari, S. D., Schwikowski, M., Gysel, M., Flanner, M. G., Kang, S., Hou, S., and Mayewski, P. A.: Recent Increase in Black Carbon Concentrations from a Mt. Everest Ice Core Spanning 1860–2000 AD, Geophys. Res. Lett., 38, L04703, doi:10.1029/2010GL046096, 2011.

Kaspari, S., Painter, T. H., Gysel, M., Skiles, S. M., and Schwikowski, M.: Seasonal and elevational variations of black carbon and dust in snow and ice in the Solu-Khumbu, Nepal and estimated radiative forcings, Atmos. Chem. Phys., 14, 8089–8103, doi:10.5194/acp-14-8089-2014, 2014.

Li, C., Bosch, C., Kang, S., Andersson, A., Chen, P., Zhang, Q., Cong, Z., Chen, B., Qin, D., and Gustafsson, Ö.: Sources of black carbon to the Himalayan-Tibetan Plateau glaciers, Nat. Commun., 7, 12574, doi:10.1038/ncomms12574, 2016a.

Li, Y., Chen, J., Kang, S., Li, C., Qu, B., Tripathee, L., Yan, F., Zhang, Y., Guo, J., Gul, C., and Qin, X.: Impacts of black carbon and mineral dust on radiative forcing and glacier melting during summer in the Qilian Mountains, northeastern Tibetan Plateau, The Cryosphere Discuss., doi:10.5194/tc-2016-32, 2016b.

Li, X., Kang, S., He, X., Qu, B., Tripathee, L., Jing, Z., Paudyal, R., Li, Y., Zhang, Y., Yan, F., Li, G., and Li, C.: Light-absorbing impurities accelerate glacier melt in the Central Tibetan Plateau, Sci. Total Environ., 587–588, 482–490, doi:10.1016/j.scitotenv.2017.02.169, 2017.

Li, X., Kang, S., Zhang, G., Qu, B., Tripathee, L., Paudyal, R., Jing, Z., Zhang, Y., Yan, F., Li, G., Cui, X., Xu, R., Hu, Z., Li, C.: Light-absorbing impurities in a southern Tibetan Plateau glacier: Variations and potential impact on snow albedo and radiative forcing, Atmos. Res., 200, 77-87, doi:10.1016/j.atmosres.2017.10.002, 2018.

Liu, X., Xu, B., Yao, T., Wang, N., and Wu, G.: Carbonaceous particles in Muztag Ata ice core, West Kunlun Mountains, China, Chinese Sci. Bull., 53, 3379–3386, 2008.

Ming, J., Cachier, H., Xiao, C., Qin, D., Kang, S., Hou, S., and Xu, J.: Black carbon record based on a shallow Himalayan ice core and its climatic implications, Atmos. Chem. Phys., 8, 1343–1352, doi:10.5194/acp-8-1343-2008, 2008.

Ming, J., Xiao, C. D., Cachier, H., Qin, D. H., Qin, X., Li, Z. Q., and Pu, J. C.: Black Carbon (BC) in the snow of glaciers in west China and its potential effects on albedos, Atmos. Res., 92, 114–123, doi:10.1016/j.atmosres.2008.09.007, 2009a.

Ming, J., Xiao, C., Du, Z., and Flanner, M. G.,: Black carbon in snow/ice of west China and its radiave forcing, Adv. Climate Change Res., 5(6), 328–35, 2009b (in Chinese with English abstract).

Ming, J., Du, Z. C., Xiao, C. D., Xu, X. B., and Zhang, D. Q.: Darkening of the mid-Himalaya glaciers since 2000 and the potential causes, Environ. Res. Lett., 7, 014021, doi:10.1088/1748-9326/7/1/014021, 2012.

Ming, J., Xiao, C. D., Du, Z. C., and Yang, X. G.: An overview of black carbon deposition in High Asia glaciers and its impacts on radiation balance, Advances in Water Resources, 55, 80–87, doi:10.1016/j.advwatres.2012.05.015, 2013.

Ming, J., Xiao, C., Wang, F., Li, Z., and Li, Y.: Grey Tienshan Urumqi Glacier No.1 and light-absorbing impurities, Environ. Sci. Pollut. R., 23, 9549–9558, doi:10.1007/s11356- 016-6182-7, 2016.

Niu, H.W., S.C. Kang, Y.L. Zhang, X.Y. Shi, X.F. Shi, S.J. Wang, et al.: Distribution of light-absorbing impurities in snow of glacier on Mt. Yulong, southeastern Tibetan Plateau, Atmos. Res., 197, 474-484, doi:10.1016/j.atmosres.2017.07.004, 2017.

Qu, B., Ming, J., Kang, S.-C., Zhang, G.-S., Li, Y.-W., Li, C.-D., Zhao, S.-Y., Ji, Z.-M., and Cao, J.-J.: The decreasing albedo of the Zhadang glacier on western Nyainqentanglha and the role of light-absorbing impurities, Atmos. Chem. Phys., 14, 11117-11128, doi:10.5194/acp-14-11117-2014, 2014.

Schmale, J., Flanner, M., Kang, S., Sprenger, M., Zhang, Q., Guo, J., Li, Y., Schwikowski, M., and Farinotti, D.: Modulation of snow reflectance and snowmelt from Central Asian glaciers by anthropogenic black carbon, Sci. Rep.-UK, 7, 40501, doi:10.1038/srep40501, 2017.

Svensson, J., Ström, J., Kivekäs, N., Dkhar, N. B., Tayal, S., Sharma, V. P., Jutila, A., Backman, J., Virkkula, A., Ruppel, M., Hyvärinen, A., Kontu, A., Hannula, H.-R., Leppäranta, M., Hooda, R. K., Korhola, A., Asmi, E., and Lihavainen, H.: Light-absorption of dust and elemental carbon in snow in the Indian Himalayas and the Finnish Arctic, Atmos. Meas. Tech., 11, 1403-1416, doi:10.5194/amt-11-1403-2018, 2018.

Wang, M., Xu, B., Kaspari, S. D., Gleixner, G., Schwab, V. F., Zhao, H., Wang, H., and Yao, P.: Century-long record of black carbon in an ice core from the Eastern Pamirs: Estimated contributions from biomass burning, Atmos. Environ., 115, 79–88, doi:10.1016/j.atmosenv.2015.05.034, 2015.

Xu, B., Yao, T., Liu, X., and Wang, N.: Elemental and organic carbon measurements with a two-step heating-gas chromatography system in snow samples from the Tibetan plateau, Ann. Glaciol., 43, 257–262, doi:10.3189/172756406781812122, 2006.

Xu, B.-Q., M. Wang, D. R. Joswiak, J.-J. Cao, T.-D. Yao, G.-J. Wu, W. Yang, and H.-B. Zhao: Deposition of anthropogenic aerosols in a southeastern Tibetan glacier, J. Geophys. Res., 114, D17209, doi:10.1029/2008JD011510, 2009a.

Xu, B. Q., Cao, J. J., Hansen, J., Yao, T. D., Joswia, D. R., Wang, N. L., Wu, G. J., Wang, M., Zhao, H. B., Yang, W., Liu, X. Q., and He, J. Q.: Black soot and the survival of Tibetan glaciers, P. Natl. Acad. Sci. USA, 106, 22114–22118, doi:10.1073/pnas.0910444106, 2009b.

Xu, B., Cao, J., Joswiak, D. R., Liu, X., Zhao, H., and He, J.: Postdepositional enrichment of black soot in snow-pack and accelerated melting of Tibetan glaciers, Environ. Res. Lett., 7, 14022, doi:10.1088/1748-9326/7/1/014022, 2012.

Yang, S., B. Xu, J. Cao, C. S. Zender, and M. Wang: Climate effect of black carbon aerosol in a TP glacier, Atmos. Environ., 111, 71–78, doi:10.1016/j.atmosenv.2015.03.016, 2015.

Zhang, Y., Kang, S., Cong, Z., Schmale, J., Sprenger, M., Li, C., Yang, W., Gao, T., Sillanpää, M., Li, X., Liu, Y., Chen, P., and Zhang, X.: Light-absorbing impurities enhance glacier albedo reduction in the southeastern Tibetan Plateau, J. Geophys. Res.-Atmos., 122, 6915–6933, doi:10.1002/2016JD026397, 2017a.

Zhang, Y., Kang, S., Li, C., Gao, T., Cong, Z., Sprenger, M., Liu, Y., Li, X., Guo, J., Sillanpää, M., Wang, K., Chen, J., Li, Y., and Sun, S.: Characteristics of black carbon in snow from Laohugou No. 12 glacier on the northern Tibetan Plateau, Sci. Total Environ., 607–608, 1237–1249, doi:10.1016/j.scitotenv.2017.07.100, 2017b.

Zhang, Y., Kang, S., Sprenger, M., Cong, Z., Gao, T., Li, C., Tao, S., Li, X., Zhong, X., Xu, M., Meng, W., Neupane, B., Qin, X., and Sillanpää, M.: Black carbon and mineral dust in snow cover on the Tibetan Plateau, The Cryosphere, 12, 413-431, doi:10.5194/tc-12-413-2018, 2018.